Relative changes in CO emissions over megacities based on observations from space

Matthieu Pommier, Chris A. Mclinden, Merritt Deete

Relative changes in CO emissions over megacities based on observations from space

Matthieu Pommier,[1,2] Chris A. McLinden,[1] and Merritt Deeter[3]

Received 19 June 2013; accepted 28 June 2013; published 26 July 2013.

[1] Urban areas are large sources of several air pollutants, with carbon monoxide (CO) among the largest. Yet measurement from space of their CO emissions remains elusive due to its long lifetime. Here we introduce a new method of estimating relative changes in CO emissions over megacities. A new multichannel Measurements of Pollution in the Troposphere (MOPITT) CO data product, offering improved sensitivity to the boundary layer, is used to estimate this relative change over eight megacities: Moscow, Paris, Mexico, Tehran, Baghdad, Los Angeles, Sao Paulo, and Delhi. By combining MOPITT observations with wind information from a meteorological reanalysis, changes in the CO upwind-downwind difference are used as a proxy for changes in emissions. Most locations show a clear reduction in CO emission between 2000–2003 and 2004–2008, reaching −43% over Tehran and −47% over Baghdad. There is a contrasted agreement between these results and the MACCity and Emission Database for Global Atmospheric Research v4.2 inventories.
Citation: Pommier, M., C. A. McLinden, and M. Deeter (2013), Relative changes in CO emissions over megacities based on observations from space, *Geophys. Res. Lett.*, *40*, 3766–3771, doi:10.1002/grl.50704.

1. Introduction

[2] A rapidly increasing global population combined with economic growth in most of the developing countries has led to an increase in urban surface area with negative consequences on global air quality. Human activities emit significant quantities of many pollutants, with carbon monoxide (CO) among them. Due to its relatively long lifetime of several weeks in the troposphere, it is used most often as a tracer of pollution transport in satellite or model studies [e.g., *Sodemann et al*., 2011]. CO is also an important precursor of ozone (O_3) through photochemical production in the presence of nitrogen oxides (NO_x). It is produced mainly from the incomplete combustion of fossil fuels by industry, car traffic or domestic heating system, and vegetation combustion or forest fires [e.g., *Badr and Probert*, 1995]. It is also produced in the atmosphere following oxidation of hydrocarbons. Since both its sources and sinks vary seasonally, CO also exhibits a seasonal cycle and has an important role in the oxidizing power of the atmosphere, influencing the concentrations of CH_4 and O_3.

[3] Despite its clear importance, monitoring CO near the surface remains a challenge. Nadir-viewing satellite instruments such as MOPITT (Measurements of Pollution in the Troposphere) [*Drummond*, 1992] provide global coverage and, thus, are a powerful tool for monitoring the pollutants. Nevertheless, for satellite trace gas products based solely on nadir thermal infrared (TIR) measurements, the vertical sensitivity is limited, particularly in the boundary layer (BL), and represents an impediment to air quality studies. However, the new MOPITT Version 5 product, combining TIR and near-infrared (NIR) observations, provides better sensitivity close to the surface, and the first studies over China [*Worden et al*., 2010, 2012] and over the United States [*Deeter et al*., 2012] showed promising results. Although MOPITT was not designed to detect local pollution plumes, *Clerbaux et al*. [2008] demonstrated that it was possible to detect the enhancement of CO over megacities if only at a resolution similar to that of the city itself. More recent studies have shown that it was possible to detect enhanced concentrations of other pollutants (NO_2 or SO_2) with an improved spatial resolution [*Fioletov et al*., 2011; *McLinden et al*., 2012], and from this, estimates of lifetime and emissions could be made [*Beirle et al*., 2011]. *Stremme et al*. [2013] also showed that satellites can improve information about CO emissions with a top-down estimation, as over Mexico.

[4] Due to large chemical sources and sinks and large-scale transport, CO concentrations in the atmosphere are not only driven by local direct emissions. *Granier et al*. [2011] highlighted the difficulties for the community to determine precisely the CO anthropogenic emissions even if more detailed studies are now available on natural emissions, as, for example, in *Fortems-Cheiney et al*. [2009]. A better estimation of anthropogenic emissions is hence a key factor in quantifying the global CO budget. Monitoring trends over urban areas, characterized by stable air masses with high enhanced concentrations of pollutants as CO (so-called urban "domes") of atmospheric carbon, may demonstrate the effect of stabilization policies of pollutant emissions.

2. MOPITT CO

2.1. MOPITT

[5] The MOPITT instrument was launched in 1999 on board the Terra satellite and has been providing nearly continuous measurements of CO since March 2000. MOPITT views the Earth over all latitudes with a pixel size of 22 km × 22 km at nadir and a cross-track swath that

Additional supporting information may be found in the online version of this article.

[1]Air Quality Research Division, Science and Technology Branch, Environment Canada, Toronto, Ontario, Canada.
[2]Now at UPMC Université Paris 06; Université Versailles St-Quentin, UMR 8190, CNRS/INSU, LATMOS-IPSL, Paris, France.
[3]Atmospheric Chemistry Division, National Center for Atmospheric Research, Boulder, Colorado, USA.

Corresponding author: M. Pommier, UPMC/LATMOS-IPSL, 4 Place Jussieu, FR-75252 Paris CEDEX 05, France. (matthieu.pommier@latmos.ipsl.fr)

0094-8276/13/10.1002/grl.50704

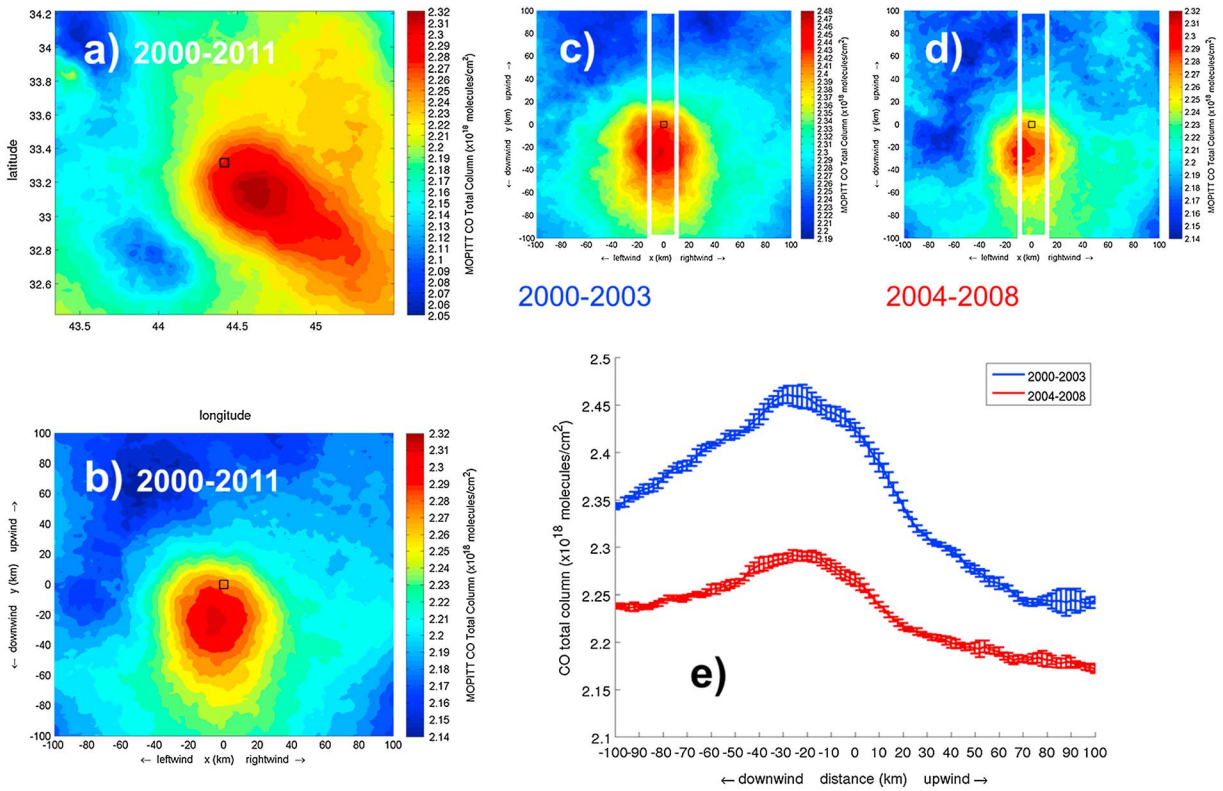

Figure 1. Mean daytime MOPITT CO total column distribution (in 10^{18} molecules/cm^2) over Baghdad from March 2000 to December 2011 shown on a 2×2 km^2 grid, calculated using an averaging radius of 28 km, (a) over a 200×200 km^2 area and (b) after rotation of all pixels in a upwind-downwind direction. The rotated distribution is also presented for the periods (c) 2000–2003 and (d) 2004–2008. The open black square in the center of the maps represents the location of the megacity. Only cloud-free scenes are used. Figure 1e shows the zonally integrated (±10 km; white box in Figures 1c and 1d) MOPITT CO total column mean after rotation of all pixels in an upwind-downwind direction over Baghdad as a function of distance of the megacities center 0. The mean value is calculated from (blue) March 2000 to December 2003 and (red) from January 2004 to December 2008, and the error bars represent the standard deviation.

measures a near-global distribution of CO every 3 days, around 10:30 A.M. (or P.M.) local time. It uses the technique of gas-filter correlation radiometry, observing simultaneously in both a TIR band near 4.7 µm and a NIR band near 2.3 µm [*Drummond et al.*, 2009]. Previous data versions utilized only the TIR channels. Recently, improved understanding of geophysical noise in the MOPITT NIR channels [*Deeter et al.*, 2011, 2013] has allowed the development of "multispectral" MOPITT products exploiting both the TIR and NIR channels. More details on this TIR + NIR new retrieval algorithm and data product are provided in *Worden et al.* [2010]. The correction employed for the geolocation bias discovered during this analysis is provided in the supporting information.

[6] Since CO has a long lifetime in the troposphere, our study is mainly applicable to remote areas or sites surrounded by mountains, thus not affected by pollution transported from other cities or biomass burning regions and additionally needs to be well contrasted with the background levels. It is also necessary to target larger urban areas such as megacities (>5 millions of inhabitants) in order to detect an enhancement. Data were screened to include only that with the highest signal-to-noise ratio, that is, over land, during daytime, locations where the conflict in the pixel between land and water is limited (i.e., not close to the coast), and cloud-free scenes (cloud fraction = 0 and cloud index = 2).

[7] This study focuses on total column CO as opposed to mixing ratio in the surface layer as the measurements often possess less than 2 degrees of freedom for signal (DFS). The strongest enhancements over the megacities were mostly found using the total column and not with the surface mixing ratio. This may be a result of the limited vertical sensitivity (close to a column), and hence, the retrieved total column exhibits smaller random errors than the surface mixing ratio. This limited sensitivity could also negate the impact of vertical transport.

2.2. Spatial Mapping

[8] CO maps are constructed using the pixel averaging technique [*Fioletov et al.* 2011] as it allows for the analysis of the long-term mean spatial CO distribution with an improved effective resolution. For this, a geographical grid (200×200 km^2), as shown in Figure S1 in the supporting information, with a 2 km step (Δx and Δy), is established around the source, and the average of all MOPITT pixels centred within a 28 km radius (r) from each grid point is calculated. The value assigned to a grid box corresponds to the average of all data within this radius. This technique thus oversamples the data, and as a result, additional details of the spatial distribution emerge. Figure 1a shows the average CO distribution over Baghdad, where winds were

Table 1. Downwind-Upwind Difference of CO Total Column Over Eight Megacities (10^{17} molecules/cm^2) Observed by MOPITT Between 2000–2003 and 2004–2008 and the RD Associated (%)[a]

Megacity (Coordinates and Population in Millions of Inhabitants[b])	$V_d - V_u$ MOPITT 2000–2003 (10^{17} molecules/cm^2)	$V_d - V_u$ MOPITT 2004–2008 (10^{17} molecules/cm^2)	RD (%)	RD MACCity (%)	RD EDGAR v4.2 (%)
Moscow (55.75°N, 37.62°E–16.3°E)	2.8 ± 0.03	2.3 ± 0.06	−18.5 ± 3.7	−10.7 ± 31.5	−12.9 ± 44.6
Paris (48.85°N, 2.35°E–10.6°E)	1.3 ± 0.05	1.0 ± 0.03	−22.2 ± 6.9	−34.9 ± 50.2	−54.4 ± 36.6
Mexico (19.4°N, 99.1°W–23.6°W)	7.0 ± 0.09	4.2 ± 0.06	−39.9 ± 2.6	+12.1 ± 48.3	−12.7 ± 42.2
Tehran (35.68°N, 51.42°E–13.8°E)	4.4 ± 0.02	2.5 ± 0.06	−42.9 ± 2.8	+6.0 ± 67.2	+4.6 ± 72.2
Baghdad (33.32°N, 44.42°E–6.4°E)	2.2 ± 0.01	1.2 ± 0.03	−46.5 ± 2.9	+3.5 ± 12.3	+11.7 ± 42.5
Los Angeles (34.05°N, 118.23°W–17.1°W)	6.1 ± 0.11	4.9 ± 0.07	−19.6 ± 3.4	−39.5 ± 29.7	−32.6 ± 31.1
Sao Paulo (23.53°S, 46.62°W–21.4°W)	1.5 ± 0.04	1.1 ± 0.03	−26.9 ± 5.4	+7.8 ± 27.5	−0.1 ± 33.1
Delhi (28.63°N, 77.22°E–23.7°E)	0.9 ± 0.02	1.1 ± 0.04	+22.4 ± 5.8	+2.7 ± 60.1	−1.8 ± 64.1

[a]The RDs for MACCity and EDGAR v4.2 emission inventories are also provided between both periods. The RDs are calculated as follows: [(CO 2004–2008 − CO 2000–2003)/CO 2000–2003] × 100. The uncertainties (statistical error) given are described in the supporting information.
[b]Source for population: http://www.citypopulation.de/world/Agglomerations.html. The reference date is 01 April 2013.

mainly coming from the northwest, i.e., ~278° (for reference, the North is at 0°).

3. Impact of Boundary Layer Wind on CO Distribution

[9] Wind speed and direction are key factors that influence the distribution of pollutants. Herein we merged ECMWF (European Centre for Medium-Range Weather Forecasts) reanalysis data (http://data-portal.ecmwf.int/data/d/interim_full_daily) averaged over altitude through the boundary layer (BL) with MOPITT observations. The BL was assigned a constant height of 700 hPa. Since this choice is somewhat arbitrary, the study was also performed using only surface winds and a BL up to 800 hPa. Each MOPITT pixel of the studied domain was associated to an ECMWF wind field represented on a 0.75° × 0.75° grid. The wind fields were interpolated spatially and temporally to the location and overpass time of each MOPITT pixel.

[10] This merging allowed for the filtering of observations according to wind direction, analogous to that used in other studies (e.g., *Beirle et al*. [2011]). The BL wind direction will influence the location of the CO maxima, while the BL wind speed impacts the length of the downwind tail (Figure S2).

[11] Instead of using this directional filtering to examine the distribution as a function of downwind distance, the approach adopted here involves a rotation of the location of each MOPITT observation about some reference points such that after rotation, all have a common wind direction (see supporting information for details). Each data point maintains its upwind-downwind character, and there is the advantage that all data, regardless of wind direction, can be analyzed together. The rotation of the MOPITT pixels effectively redistributes the observations over the megacity along the upwind-downwind direction. This is shown in Figure 1b for Baghdad, where a clear contrast is observed between the upwind and downwind directions. Figures 1c and 1d show the same distribution for 2000–2003 and 2004–2008, respectively. A difference in the intensity of the enhancement between both periods is noted, highlighting higher values and a larger plume during 2000–2003. The enhancement is located in a downwind area as a result of our rotation of the MOPITT pixels. A sharper contrast between the upwind and downwind areas appears to be linked to the BL wind speed. Baghdad, which had a large BL wind speed (6.5 m/s) (Table S1) compared to the mean of the megacities studied (5.1 m/s), presents clearly a new distribution. In contrast, this effect is weaker for cities with slower BL wind speed, as Mexico (2.5 m/s) (Figure S2). Thus, a higher BL mean wind speed introduces a higher contrast between the upwind and downwind areas, in spite of this limited effect on the original CO distribution (Figure S3).

4. Changes in Megacity CO Emissions

4.1. Estimates Using MOPITT

[12] An examination of the downwind-upwind differences was used to derive information on the estimate CO emission trends from the eight selected megacities. The first step in this process was calculating the cross-wind average CO total column, as shown in Figure 1e for Baghdad over a 4 year interval and a 5 year interval, i.e., 2000–2003 and 2004–2008, respectively. This graph confirms the decrease in CO total column observed on both maps (Figures 1c and 1d). The averaging zone (±10 km from the center line) was chosen to include the main CO enhancement. The upwind CO total column values can be interpreted as the background distribution. If the downwind-upwind difference is assumed to be proportional to the megacity emissions, then the relative difference (RD) in the downwind-upwind difference between these two periods can be taken as an estimate of the relative change in emissions, as summarized in Table 1. Thus, we average five maximum CO total columns (downwind) and five minimum CO total columns (upwind) as follows:

$$\text{downwind-upwind difference} = V_d - V_u = \frac{\sum_{i=1}^{5} \max(\text{COtot}\,i\,\text{downwind})}{5} - \frac{\sum_{i=1}^{5} \min(\text{COtot}\,i\,\text{upwind})}{5} \quad (1)$$

[13] The RD has an uncertainty and an error budget associated with it. The uncertainty corresponds to a statistical error. It is described in the supporting information, and the results are summarized in Table 1. The error budget is given in the supporting information, but it is based on the sensitivity of these estimates to several chosen parameters such as the averaging radius of the circle, the size of the grid, the across-wind averaging distance, and the BL height (Table S3). The budget error varies widely among the different locations. The parameters used have a large influence over Paris, Sao Paulo, and Delhi, but they are negligible over Baghdad or Mexico. Baghdad and Mexico are more isolated from regional sources than the three other megacities, probably explaining the

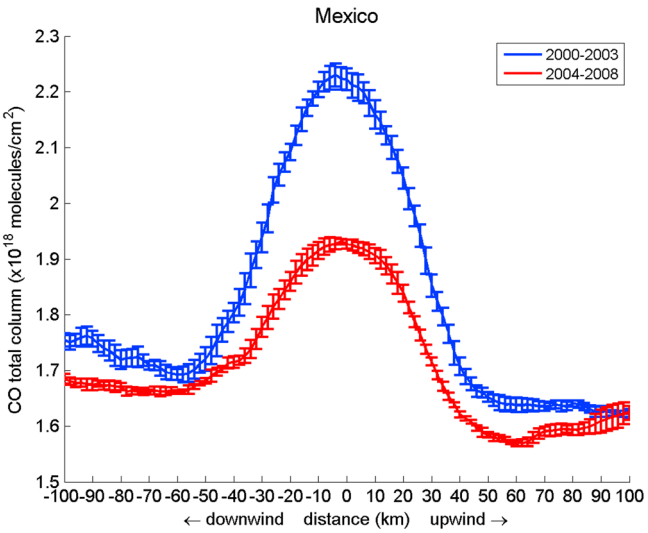

Figure 2. Zonally integrated (±10 km) MOPITT CO total column mean (in 10^{18} molecules/cm^2) after rotation of all pixels in an upwind-downwind direction over Mexico as a function of distance of the megacities center 0. The error bars correspond to the standard deviation.

lowest errors due to the criteria as the radius, the size of the grid, and the across-wind averaging distance.

[14] Due to small average wind speeds, the distribution over Mexico was only marginally affected by the rotation (Figure S2), highlighting the existence of a "CO dome" over the city (Figure 2).

4.2. Comparisons With Emission Inventories

[15] The selected periods were chosen to match with the emission inventories used (Table 1) so that comparisons can be made in order to assess their consistency. The two considered here are the MACCity (MACC/CityZEN EU projects) anthropogenic emissions inventory (1990–2010, at a 0.5° grid for 19 species) [*Granier et al*., 2011] and the Emission Database for Global Atmospheric Research (EDGAR) v4.2 inventory (1970–2008 and has a 0.1° grid) [*Janssens-Maenhout et al*., 2010]. In MACCity, a data set was created, based on the 1990 and 2000 Atmospheric Chemistry and Climate Model Intercomparison Project (ACCMIP) emissions and the 2005 and 2010 emissions provided by Representative Concentration Pathways (RCP) 8.5 (see http://ether.ipsl.jussieu.fr/eccad for both inventories). The emissions for each compound were linearly interpolated, for each sector (in total, 10 anthropogenic sectors such as agricultural, energy, etc.) and each year between 2000 and 2005 and for each year between 2005 and 2010 based on these ACCMIP and RCP emissions, while in EDGAR v4.2, they were calculated each year. We have to keep in mind this difference between both inventories in our comparison for both periods since it should introduce a bias in the calculated trend.

[16] Emissions from both inventories were averaged over an area of 0.25° × 0.25° around the location of each megacity, as given in Table S2. This was done for both periods, and their RD was computed with these values also given in Table 1. The agreement in the RDs between the two inventories was mixed. Most locations had RDs in emissions that were consistent, to within 10%, but larger (≥30%) RDs were found for Los Angeles (LA) and Paris. This illustrates the impact of some of the errors associated with the size of the grid and the reference years for the update of the inventories in our RD calculation [e.g., *Lopez et al*., 2013]. An analysis of the sensitivity of these to the summation area and period studied was conducted, as summarized in the supporting information (Tables S4 and S5). Both inventories had error budgets that agreed: over Tehran and Sao Paulo, values were very large (>100%), while over LA, the error with EDGARv4.2 is negligible (0.3%).

[17] We can note that with our proxy, a megacity as Paris emitted roughly the same amount of CO between 2004 and 2008 than Delhi between 2000 and 2003 (1.0 and 0.9×10^{17} molecules/cm^2, respectively). Paris shows a reduction in CO total column compared to 2000–2003 (−22%), while Delhi presents a large increase (+22.4%) (Table 1). Over Europe as a whole, this decrease began with the invention (in 1975) and mandatory application (in 1993) of catalytic converters and the growth of diesel engine vehicle market share [*Wang et al*., 2012]. There may also be some connection to the 2008 economic crisis as explained by *Castellanos and Boersma* [2012], who observed a modification of the regional NO_x concentrations due to changes in the economy in Europe, even if this crisis overlaps only the last year of our studied period. The reduction in CO over Europe was already noted by *Worden et al*. [2013], using the MOPITT data. Both inventories also present a negative trend over Paris, while they disagree for Delhi, and the absolute values of these trends are strongly underestimated compared to our proxy based on the MOPITT observations. Sao Paulo lies in the same category as Paris, with similar values of CO total columns for both periods and the same negative trend, but its population is more similar to that of Mexico or Delhi. EDGARv4.2 also presents a slight decrease, where MACCity shows a positive trend. The downwind-upwind total column difference over Baghdad was the same as over Delhi in 2004–2008 (1.2 and 1.1×10^{17} molecules/cm^2, respectively), but Baghdad shows a decrease between both periods, unlike Delhi. Baghdad, which is the smaller city, shows the larger decrease in all sites studied compared to 2000–2003 (−46.5%), unlike the inventories emissions. The reduction in CO over Tehran (−42.9%) is similar to that over Baghdad or Mexico, while the decrease in CO over Moscow is comparable to LA (~ −20%). The decrease in CO over Moscow was already observed by *Rakitin et al*. [2011] with ground measurements. Mexico and LA are the most polluted megacities over both periods despite a large reduction in the total column difference (−39.9% and −19.6%, respectively). Over LA, both inventories show the same trends as MOPITT, but they are overestimated by 1/3 with EDGARv4.2 and by 1/2 with MACCity. Both inventories do not present the same trend over Mexico. MACCity gives a positive trend, as opposed to the negative trend derived from the MOPITT observations. The CO decrease over LA is also in agreement with the study by *Parrish et al*. [2011], showing that over the last five decades, air quality in North American megacities has improved substantially despite substantial increases in population and vehicle traffic, and by *Warneke et al*. [2012], showing a reduction in CO of 7.8%/yr for the LA basin. The reduction over LA may be linked, but not fully explained, to initiation of the city in a program in 2007 to cut greenhouse gas emissions to 35% below 1990 levels by 2030 (see http://www.ci.la.ca.us/ead/pdf/GreenLA_CAP_2007.pdf). The RD between 2000–2003 and

2004–2007 over LA was only 12%, showing the large decrease in emission during 2008. It could be also linked, as for Paris, to the economic crisis [*Russell et al*., 2012].

[18] Except over Delhi, a clear reduction in CO was observed by MOPITT. This reduction in emission decreases their impact on the global CO background levels. It is linked to reductions of fossil fuel emissions as the reduction in the land transportation category with smaller decreases in land use and energy, industry, and waste [*Hemispheric Transport of Air Pollution*, 2010]. It was also already noticed over the United States by the Environmental Protection Agency (see http://www.epa.gov/air/airtrends/carbon.html) and in regional studies as *Granier et al*. [2011], except in Asia. Nevertheless, for China, in the study by *Granier et al*. [2011], they used the updated emissions in 2006 from *Zhang et al*. [2009] but likely did not consider more recent updates to activity data in China such as the inventory used to model CO emissions before and during the 2008 Beijing Olympics [*Worden et al*., 2012]. *Worden et al*. [2012] observed over Beijing reductions in CO emissions by 2008 (even without considering the reductions from restrictions during the Olympics) due to such measures as stricter vehicle emission standards, phasing out of residential coal stove use, and changes in the industry sector. Globally, a major problem using global inventories to represent urban-scale emissions is their coarse resolution. With the inventories, it is difficult to distinguish the emissions from urban area and the background levels, but it stays the best way to get the climatology over worldwide cities.

5. Conclusions

[19] This study represents a first attempt to use remote sensing measurements to determine relative change in CO emissions over megacities. Satellite data can be used for this estimation without any assimilation or modeling process, costly in terms of run time.

[20] Air quality studies based on a nadir-viewing instrument and TIR measurements are challenging due to the limited vertical sensitivity close to the surface, but we showed that we can monitor high CO concentrations over megacities as Baghdad. Nevertheless, due to the MOPITT characteristics, our study is only applicable over a large urban area and over land, during daytime, and which is not influenced by other sources.

[21] Based on previous studies, we combined the BL wind information from ECMWF reanalysis with a new pixel averaging technique, highlighting changes in the CO downwind-upwind difference. These are used as a proxy for changes in emissions. This method seems more relevant for cities with higher mean BL wind speeds. Over most of the selected sites, a clear reduction in CO emission is observed between the two periods, 2000–2003 and 2004–2008, but with a limited agreement with two different inventories. This decrease ranges between ~19% over Moscow and ~47% over Baghdad. Delhi exhibits significant increased emissions during the 2004–2008 period (+22.4%) but with a reasonable amount of CO (1.1×10^{17} molecules/cm^2) comparable to the amount emitted by Baghdad, Paris, and Sao Paulo. This reduction in CO over cities could impact the budget of secondary pollutants as ozone [e.g., *Pollack et al*., 2013].

[22] **Acknowledgments.** M. Pommier was supported by a fellowship grant from the Natural Sciences and Engineering Research Council of Canada (NSERC, Canada). We thank the NASA for the free use of the MOPITT data (ftp://l4ftl01.larc.nasa.gov/) and the ETHER Data Center for the free access to emission inventories via ECCAD (http://ether.ipsl.jussieu.fr/eccad).

[23] The Editor thanks two anonymous reviewers for their assistance in evaluating this paper.

Reference

Badr, O., and S. D. Probert (1995), Carbon monoxide concentration in the Earth's atmosphere, *Appl. Energy*, *50*(4), 339–372.

Beirle, S., et al. (2011), Megacity emissions and lifetimes of nitrogen oxides probed from space, *Science*, *333*, 1737–1739, doi:10.1126/science.1207824.

Castellanos, P., and K. F. Boersma (2012), Reductions in nitrogen oxides over Europe driven by environmental policy and economic recession, Sci. Rep., 2, 265, 1–7, doi:10.1038/srep00265, 2012.

Clerbaux, C., et al. (2008), Carbon monoxide pollution from cities and urban areas observed by the Terra/MOPITT mission, *Geophys. Res. Lett.*, *35*, L03817, doi:10.1029/2007GL032300.

Deeter, M. N., et al. (2011), MOPITT multispectral CO retrievals: Origins and effects of geophysical radiance errors, *J. Geophys. Res.*, *116*, D15303, doi:10.1029/2011JD015703.

Deeter, M. N., et al. (2012), Evaluation of MOPITT retrievals of lower-tropospheric carbon monoxide over the United States, *J. Geophys. Res.*, *117*, D13306, doi:10.1029/2012JD017553.

Deeter, M. N., et al. (2013), Validation of MOPITT Version 5 thermal-infrared, near-infrared, and multispectral carbon monoxide profile retrievals for 2000–2011, *J. Geophys. Res. Atmos.*, 1–16, doi:10.1002/jgrd.50272.

Drummond, J. R. (1992), Measurements of Pollution in the Troposphere (MOPITT), in *The Use of EOS for Studies of Atmospheric Physics*, edited by J. C. Gille and G. Visconti, pp. 77–101, North-Holland, New York.

Drummond, J. R., et al. (2009), A review of 9-year performance and operation of the MOPITT instrument, *Adv. Space Res.*, *45*, 760–774, doi:10.1016/j.asr.2009.11.019.

Fioletov, V. E., et al. (2011), Estimation of SO_2 emissions using OMI retrievals, *Geophys. Res. Lett.*, *38*, L21811, doi:10.1029/2011GL049402.

Fortems-Cheiney, A., et al. (2009), On the capability of IASI measurements to inform about CO surface emissions, *Atmos. Chem. Phys.*, *9*, 8735–8743, doi:10.5194/acp-9-8735-2009.

Granier, C., et al. (2011), Evolution of anthropogenic and biomass burning emissions of air pollutants at global and regional scales during the 1980–2010 period, *Clim. Change*, doi:10.1007/s10584-011-0154-1.

Hemispheric Transport of Air Pollution (2010) New York and Geneva, Air Pollution Studies 17, Economic Commission for Europe.

Janssens-Maenhout, G., et al. (2010), Verifying greenhouse gas emissions: Methods to support international climate agreements, Greenhouse Gas Meas. Manage., 124, doi:10.1080/20430779.2011.579358.

Lopez, M., et al. (2013), Isotope- and tracer-based measurements of fossil fuel and biospheric carbon dioxide in Paris during winter 2010, *Atmos. Chem. Phys. Discuss.*, *13*, 2371–2414, doi:10.5194/acpd-13-2371-2013.

McLinden, C. A., et al. (2012), Air quality over the Canadian oil sands: A first assessment using satellite observations, *Geophys. Res. Lett.*, *39*, L04804, doi:10.1029/2011GL050273.

Parrish, D. D., et al. (2011), Air quality progress in North American megacities: A review, *Atmos. Environ.*, *45*, 7015–7025, doi:10.1016/j.atmosenv.2011.09.039.

Pollack, I. B., et al. (2013), Trends in ozone, its precursors, and related secondary oxidation products in Los Angeles, California: A synthesis of measurements from 1960 to 2010, *J. Geophys. Res. Atmos.*, *118*, 1–19, doi:10.1002/jgrd.50472.

Rakitin, V. S., E. V. Fokeeva, E. I. Grechko, A. V. Dzhola, and R. D. Kuznetsov (2011), Variations of the total content of carbon monoxide over Moscow megapolis, *Izv., Atmos. Oceanic Phys.*, *47*, 59–66, doi:10.1134/S0001433810051019.

Russell, A. R., L. C. Valin, and R. C. Cohen (2012), Trends in OMI NO_2 observations over the United States: Effects of emission control technology and the economic recession, *Atmos. Chem. Phys.*, *12*, 12,197–12,209, doi:10.5194/acp-12-12197-2012.

Sodemann, H., et al. (2011), Episodes of cross-polar transport in the Arctic troposphere during July 2008 as seen from models, satellite, and aircraft observations, *Atmos. Chem. Phys.*, *11*, 3631–3651, doi:10.5194/acp-11-3631-2011.

Stremme, W., et al. (2013), Top-down estimation of carbon monoxide emissions from the Mexico Megacity based on FTIR measurements from ground and space, *Atmos. Chem. Phys.*, *13*, 1357–1376, doi:10.5194/acp-13-1357-2013.

Wang, Z., et al. (2012), The isotopic record of Northern Hemisphere atmospheric carbon monoxide since 1950: Implications for the CO budget, *Atmos. Chem. Phys.*, *12*, 4365–4377, doi:10.5194/acp-12-4365-2012.

Warneke, C., et al. (2012), Multiyear trends in volatile organic compounds in Los Angeles, California: Five decades of decreasing emissions, *J. Geophys. Res.*, *117*, D00V17, doi:10.1029/2012JD017899.

Worden, H. M., et al. (2010), Observations of near-surface carbon monoxide from space using MOPITT multispectral retrievals, *J. Geophys. Res.*, *115*, D18314, doi:10.1029/2010JD014242.

Worden, H. M., et al. (2012), Satellite-based estimates of reduced CO and CO_2 emissions due to traffic restrictions during the 2008 Beijing Olympics, *Geophys. Res. Lett.*, *39*, L14802, doi:10.1029/2012GL052395.

Worden, H. M., et al. (2013), Decadal record of satellite carbon monoxide observations, *Atmos. Chem. Phys.*, *13*, 837–850, doi:10.5194/acp-13-837-2013.

Zhang, Q., et al. (2009), Asian emissions in 2006 for the NASA INTEX-B mission, *Atmos. Chem. Phys.*, *9*, 5131–5153.